Human Skin Gloss Perception Based on Texture Statistics

Jing Wang, Carla Kuesten, Jim Mayne, Gopa Majmudar, and Thrasyvoulos N. Pappas, *Fellow, IEEE*

***Abstract*—We propose objective, image-based techniques for quantitative evaluation of facial skin gloss that is consistent with human judgments. We use polarization photography to obtain separate images of surface and subsurface reflections, and rely on psychophysical studies to uncover and separate the influence of the two components on skin gloss perception. We capture images of facial skin at two levels, macro-scale (whole face) and meso-scale (skin patch), before and after cleansing. To generate a broad range of skin appearances for each subject, we apply photometric image transformations to the surface and subsurface reflection images. We then use linear regression to link statistics of the surface and subsurface reflections to the perceived gloss obtained in our empirical studies. The focus of this paper is on within-subject gloss perception, that is, on visual differences among images of the same subject. Our analysis shows that the contrast of the surface reflection has a strong positive influence on skin gloss perception, while the darkness of the subsurface reflection (skin tone) has a weaker positive effect on perceived gloss. We show that a regression model based on the concatenation of statistics from the two reflection images can successfully predict relative gloss differences.**

***Index Terms*—Gloss perception, multimodal photography, surface reflection, subsurface reflection**

I. Introduction

Gloss is a key perceptual attribute of visual texture that provides important information for material identification and characterization. Human skin gloss, in particular, provides information about the skin condition, for example, whether it is dry, oily, sweaty, but also about its across-sensation impression as vibrant, fresh, and healthy. The goal of this paper is to develop texture-based techniques for the objective evaluation of perceived gloss. This is important for cosmetology and can play a key role in product development, marketing, consultation, and treatment. In addition, skin gloss is important for dermatology, as it provides useful information for skin health and overall well being. For example, a number of studies [1]–[4] have shown that the appearance of matte and dull skin may be a reflection of fatigue, nutrition deficiency, hormonal imbalance, organ dysfunction, pollution, etc.

Existing techniques for quantitative measurement of skin gloss are mostly at the physical level using optical instruments like the Skin-GlossyMeter GL 200, SkinGlossMeter, Brillanometer and GonioLux. Jeudy *et al.* [5] summarize the physical models on which each instrument is based. Typically, such instruments include a probe that can be pressed at one or more locations of the skin and record the amount of reflected light in terms of gloss units (GU) based on international ISO, ASTM and DIN standards [6]. However, such measurements do not correlate well with perceived gloss. This is because the SkinGlossMeter records light specularly reflected from the skin surface at the same angle as the incident angle of the built-in red semiconductor diode laser. Thus, it does not account for variations due to the geometry of the skin surface, the orientation of the incident light, and internal reflections, all of which affect visual perception. Moreover, the probing results vary from point to point across the facial skin, and it is not clear how they jointly contribute to overall gloss perception. In contrast, in this paper we present image-based techniques that relate gloss perception to statistics of visual texture.

In general, texture appearance depends on the intrinsic material properties (light reflectivity, absorbance, transmittance), the surface geometry, the illumination, and the viewing angle [7]. The appearance of the facial skin, and gloss in particular, is especially complicated due to the multi-layer structure of the skin and the fact that it is perceived at different scales.

As illustrated in Figure 1, at the macro-scale level, gloss perception is an overall judgment that considers all the visible regions of the face including the cheeks, forehead, nose, and lips, while at the meso-scale level, gloss is evaluated at a skin patch, where pores and wrinkles are visible. We will consider gloss perception of the two scales separately.

The multi-layer structure of the skin is illustrated in Figure 2. The stratum corneum, the outer layer of the skin, is translucent and only partially reflects incident light, while the rest of the light is transmitted through, scattered by, or absorbed in the inner skin layers (epidermis and dermis). The scattered component exits the skin as reflected light in random directions. Thus, the reflection from human skin consists of a surface reflection and a subsurface reflection component. Understanding the distinct effects of these two components is important in the study of skin appearance [8].

To separate the surface and subsurface reflections of the facial skin, we rely on polarized light photography, which has been used to study skin texture, skin complexion, and radiance [3], [9]–[11]. Based on the orientation of the polarizers in front of the light source and the camera (parallel or perpendicular to each other), we can separate the surface reflection from

Manuscript received November 21, 2019; revised September 16, 2020; accepted December 1, 2020. Date of publication March 1, 2021; date of current version March 17, 2021. This article was presented in part at the IS&T Conference on Human Vision and Electronic Imaging, Burlingame, CA, USA, in 2017. The associate editor coordinating the review of this manuscript and approving it for publication was Prof. Damon M. Chandler. (Corresponding author: Thrasyvoulos N. Pappas.)

Jing Wang was with the Department of Electrical and Computer Engineering, Northwestern University, Evanston, IL 60208 USA. She is now with Bloomberg LP, New York, NY 10022 USA.

Carla Kuesten is with Amway, Ada, MI 49355 USA.

Jim Mayne, retired, was with Amway, Ada, MI 49355 USA. He is now with Integral Consultancy LLC, Greater Grand Rapids, MI, USA.

Gopa Majmudar was with Amway, Ada, MI 49355 USA. She is now with the University of Toledo, Toledo, OH 43606, USA.

Thrasyvoulos N. Pappas is with the Department of Electrical and Computer Engineering, Northwestern University, Evanston, IL 60208 USA (e-mail: pappas@ece.northwestern.edu).

Digital Object Identier 10.1109/TIP.2021.3061276

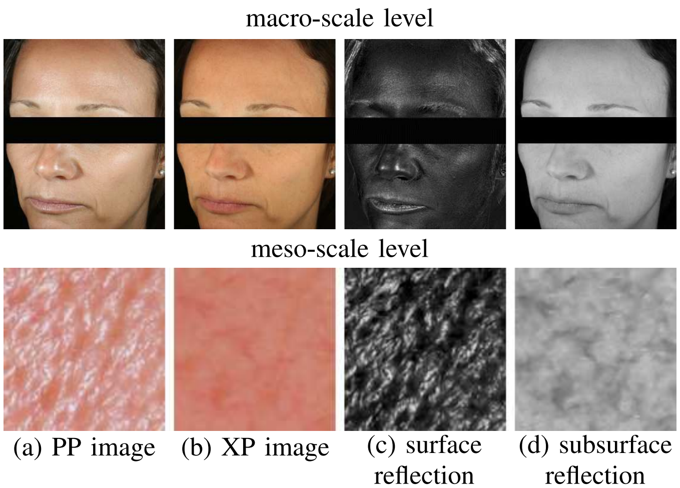

Fig. 1: Examples of polarized imaging

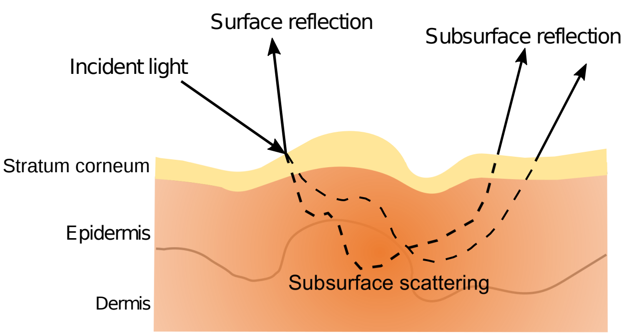

Fig. 2: Light reflections by the human skin

the subsurface reflection by subtracting the cross-polarized (XP) image (subsurface only) from the parallel-polarized (PP) image (surface and subsurface). In our analysis we use the lightness of the two reflections. Figure 1 shows examples of the PP and XP images and the lightness of the surface and subsurface reflections, at the macro-scale and meso-scale levels.

Using polarization photography, we built a human facial skin dataset by capturing high resolution facial images of 25 different subjects in two conditions, before and after cleansing. Since human skin appearance has limited variations within each subject, we enriched the dataset using photometric image transformations to simulate new appearances. We applied the S-curve transformation [12] to the surface reflection and the λ-curve transformation [13] to the subsurface reflection. Each transformation has a monotonic effect on the image histogram: the S-curve changes the contrast keeping the mean lightness unchanged, while the λ-curve has a distinct effect on the mean lightness, which changes the perceived complexion of the skin images. The two transformations change both the image statistics and the image appearance, thus allowing us to obtain additional data for exploring the relationship between statistical features of the texture image and gloss perception.

Using the expanded dataset, we designed empirical studies to uncover and separate the influence that manipulations of the surface and subsurface reflections have on skin gloss perception. Since the appearance of different subjects varies in multiple aspects, and it is difficult to manipulate each aspect independently, the focus of our initial studies was on within-subject gloss perception, that is, on visual differences among images of the same subject. We conducted separate studies at the macro-scale level (whole face) and the meso-scale level (local skin patch). Our analysis shows that the contrast of the surface reflection has a strong positive influence on skin gloss perception. Keeping the surface reflection constant, a darker skin tone in the subsurface reflection tends to result in glossier appearance. However, the differential effect of skin tone on perceived gloss diminishes when the average lightness is low. We then compared the statistics of the surface and subsurface reflection images to the results of the subjective evaluations. We found that the statistics of both the surface and subsurface reflections have a strong effect on gloss perception, even though, in some cases, the corresponding statistics (average lightness, skewness, and cluster shade) of the two reflection images have opposite effects on gloss perception. We then learned a regression model based on the concatenation of statistics from the two reflection images to predict relative gloss differences. As expected, the model that is based on statistics from surface and subsurface reflections correlates better with human judgments than the model that is based on similar statistics extracted from a single modality (overall reflection).

In summary, the focus of this paper is on the development of texture-based techniques for the objective evaluation of perceived gloss of human facial skin. The key contributions are

- The analysis of the effects of manipulation of the surface and subsurface reflections on gloss perception, at both the macro-scale and the meso-scale levels.
- The development of models based on statistical features of the surface and subsurface reflection images for the within-subject prediction of gloss perception.
- The quantitative prediction of relative gloss differences of human skin before and after cleansing.

A. *Review of existing work on gloss perception*

The relationship between image-based cues and gloss perception has been a focus of research during the past decade. Motoyoshi *et al.* [14] showed that darker and glossier appearance of a surface tends to correspond to a more positively skewed luminance histogram. Their skewness hypothesis was later challenged by several studies [15], [16], which found that the correlation between skewness and gloss perception only exists with certain lightness and texture surface restrictions.

To identify additional image-based cues, several studies utilized carefully controlled computer generated surfaces for psychophysical tests. Marlow *et al.* [17] found that specular sharpness, highlight coverage, and specular contrast correlate closely with gloss perception. Through the analysis of surface geometry, Ho *et al.* [18] found that increasing the stretch of surface relief height can change the surface gloss appearance. The relations among geometrical height relief, skewness, and gloss perception were further studied by Wijntjes and Pont [13] for Lambertian surfaces. They found that, for near-frontal illumination, skewness positively correlates with the surface relief stretch of Lambertian surfaces, which mediates visual gloss; however, this does not extend to oblique illumination. Thus, the skewness hypothesis does not lead to a complete explanation of visual gloss ratings. Lambertian surfaces were also used by Qi *et al.* [19] for the study of the relation between roughness and gloss at different spatial scales. They found complex non-linear interactions in the effects of two roughness parameters on visual gloss. Most of the work we discussed in this section, has relied on simple synthetic objects, or surfaces rendered based on reflection models in computer graphics. However, the image-based cues such work considered and their effects on gloss perception do not necessarily extend to images of real world materials [12], as the appearance of real world materials involves more complicated optical properties and physical processes.

Compared to synthetic or computer-rendered images, the study of images of real materials is hindered by the difficulty of incrementally varying image appearance. Although Motoyoshi *et al.* [14] used images of real objects in their study, the stimuli they built and the viewing conditions were quite constrained. A wider range of images of natural surfaces were investigated by Wang *et al.* [12] and in the recent work of Wiebel *et al.* [20]. To obtain a variety of controlled variations in image appearance, Wang *et al.* [12] proposed the use of the S-curve and λ-curve [13] transformations to manipulate texture lightness. Similarly, Wiebel *et al.* [20] used histogram manipulations to study the relation between contrast and gloss. Both studies found that contrast manipulation has a stronger effect on perceived gloss than skewness. However, they also found that a single statistic like skewness or contrast is not sufficient for predicting visual gloss.

To obtain a better understanding of the relationship between natural image statistics and perceived gloss, we focus on just one material, facial skin, with a rich set of statistics and appearance variations. For translucent materials, like human skin, we found that the statistical features of a single modality (overall reflection) cannot adequately account for gloss perception. Thus, we investigated the influence of the statistics of images that originate from different skin layers on the overall perception of gloss.

II. Method

A. Skin optics and polarization imaging

As discussed in the introduction, the human skin is a translucent material composed of multiple layers. The stratum corneum consists of a mixture of sebum, lipids, and sweat, and is the outer cover of the skin. When incident light reaches the skin, it is either reflected by the stratum corneum as surface reflection, or propagates into the inner layers (epidermis and dermis) of the skin tissue and reemerges as subsurface reflection. When the incident light is polarized, the surface reflection is polarized in the same direction as the incident light. Due to scattering, the subsurface reflection is undirectional.

To capture the visual data for our empirical studies, we used the VISIA-CR 4.1 Complexion Analysis System (Canfield Scientific, Parsippany, NJ), which is equipped with multiple filters to simulate different lighting modalities. In our studies we used two lighting modes: parallel-polarized (PP) and cross-polarized (XP). To capture these modes, the system uses two polarizing filters, one located in front of the source illumination and the other located in front of the camera lens. The planes of polarization of the two filters are oriented parallel (PP mode) or perpendicular (XP mode) to each other. An example of a PP image and an XP image of one subject is illustrated in Figures 1(a) and 1(b).

In the XP mode, the two filters are perpendicular to each other, and thus, all of the polarized surface reflection is removed, and only the unpolarized subsurface reflection is captured, revealing the complexion (skin redness or paleness, color heterogeneity, etc.). In the PP mode, the two filters are parallel to each other, and thus, the surface reflection component is preserved, but so is the unpolarized subsurface reflection. Since the polarization of the subsurface reflection is equally distributed in all directions, the subsurface component remains the same in both modes. Thus, the surface reflection can be obtained as the difference between the PP and XP modes (PP$-$XP), while the subsurface reflection is obtained directly from XP. Figures 1(c) and 1(d) show the separated surface and subsurface reflection components. Note that the chrominance has been removed from the two components, but can be added back after the photometric transformations.

We collected PP and XP full-face images from 25 different subjects with self-perceived oily skin. Images were obtained in frontal and side view, and in two skin conditions, before and after cleansing, for each subject. The image resolution was 590×500 pixels. We also selected multiple skin patches from different regions of the macro-scale images to obtain sets of meso-scale images with resolution 256×256 pixels.

B. Surface and subsurface manipulation

The original facial skin images of the 25 subjects we collected are insufficient to study the relationship between image-based cues and perceived gloss because they have very limited variations: before and after skin cleansing, front and side view for each subject. To increase the size of the database and to enrich the appearance range, we used two photometric transformations to independently manipulate the extracted surface and subsurface reflection images. As we mentioned above, the S-curve transformation [12] increases the contrast of an image, while the λ-curve transformation [13] changes the lightness of an image. Both modify the image histogram, which has an effect on both the appearance and the statistics of the resulting image [12], [13], thus enriching the data for the study of image-based features and their effect on image appearance. The curves are defined as follows

$$\lambda\text{-curve: } I_{out} = \sqrt{\frac{I_{in}^2}{I_{in}^2 + \lambda^2(1 - I_{in}^2)}} \quad (1)$$

$$S\text{-curve: } I_{out} = \mu - \frac{\mu - I_{in}}{\sqrt{\alpha^2(\mu - I_{in})^2(1 - 1/S^2) + 1/S^2}}, \quad (2)$$

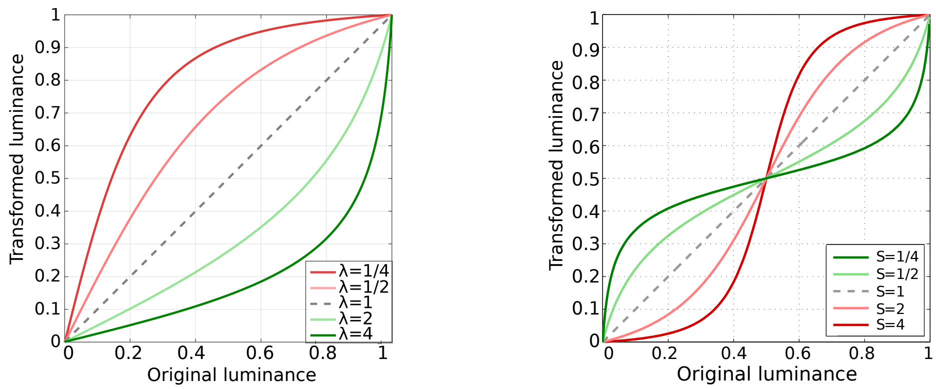

(a) λ-curves, varying λ (b) S-curves, $\mu = 0.5$, varying S

Fig. 3: Luminance transform of (a) λ-curves with varying λ and (b) S-curves with varying S

where I_{in} and I_{out} are the input and output luminance intensity values, α is defined as follows

$$\alpha = \begin{cases} \frac{1}{1-\mu}, & \text{if } I_{in} > \mu \\ \frac{1}{\mu}, & \text{if } I_{in} \leq \mu \end{cases} \tag{3}$$

and μ denotes the mean luminance. Note that both curves have a controlling parameter (S or λ) that monotonically changes the curve shape and its effect. To guarantee the output has the same mean lightness as the input luminance, the value of μ in the S-curve is determined by the mean lightness of the original luminance. Figure 3 shows how the two curves change with varying parameters.

To isolate the effects of the surface and subsurface reflections on perceived gloss, we applied the λ-curve to the surface reflection leaving the subsurface reflection unaltered, and also applied the S-curve to the subsurface reflection leaving the surface reflection unaltered. The processing steps are shown in Figure 4, and the resulting images in Figure 5. As we discussed, using polarized photography, the original surface reflection (SurfRefl) can be separated from the subsurface reflection (SubsurfRefl) by subtracting the XP from the PP lightness component (PP−XP), while the XP lightness component consists of just the subsurface reflection (SubsurfRefl). In addition, the chrominance of the surface and subsurface reflections is removed, and added back after the transformations.

For the macro-scale images, we found that it is important to exclude the non-skin regions (background, hair, eyebrows, lips, eyes, nostrils) as the application of the transformations to these regions results in unnatural appearance. For this, we used an off-the-shelf face landmark detection algorithm [21] and a color distribution algorithm [22], to obtain a binary facial mask that indicates which regions should be transformed, as illustrated in Figure 5b. Figures 5d and 5g show the results of the transformations on the surface and subsurface luminance, respectively. The two modified reflection luminances were then added up, and combined with the chrominance to obtain the final output PP image, shown in Figure 5h, which was used in the subjective studies. Note that the output XP image in Figure 5e is shown for illustrative purposes; it was not used in our studies.

TABLE I: Visual Stimuli for Empirical Study 1

		Macro-scale	**Meso-scale**
Facial skin subjects		25	12
Conditions	Lighting	PP	PP
	Viewing	Side	Side
	Cleansing	Before/After	Before/After
Each condition: 11 images (1 orig. + 10 modified SurfRefl)			
Each trial: 22 images (Before + After cleansing images of ONE skin subject in ONE view)			

The same processing was applied meso-scale facial skin images to generate multiple appearance variations.

III. Empirical Studies: Material and Methods

Given the expanded sets of data (original and modified) at the meso-scale and the macro-scale levels, we conducted separate empirical studies for determining the influence of the surface and subsurface reflection on skin gloss perception.

A. *Gloss perception versus surface reflection*

The first set of studies was intended to determine the influence of the surface reflection and was conducted with fixed subsurface reflection.

1) Visual Stimuli: The visual stimuli for Study 1A included images of 25 subjects at the macro-scale level, and the stimuli for Study 1B included 12 skin image patches at the meso-scale level. The subjects in our studies had mainly fair and light skin tones (1-3 in the Fizpatrick scale). Our studies did not cover darker skin tones (4-6 in the Fitzpatrick scale). The stimuli for both studies consisted of side view facial images. Both scales consisted of original and modified PP images of facial skin, in two skin conditions, before and after cleansing, with a cleanser specially formulated for the face. The effects of various cosmetics or treatments beyond basic cleansing that may influence the glossy appearance of the skin (toners, lotions, creams, emulsions, cleansing mousses, cleansing oils, and make-up removers) are beyond the scope of our studies. In addition, we did not consider

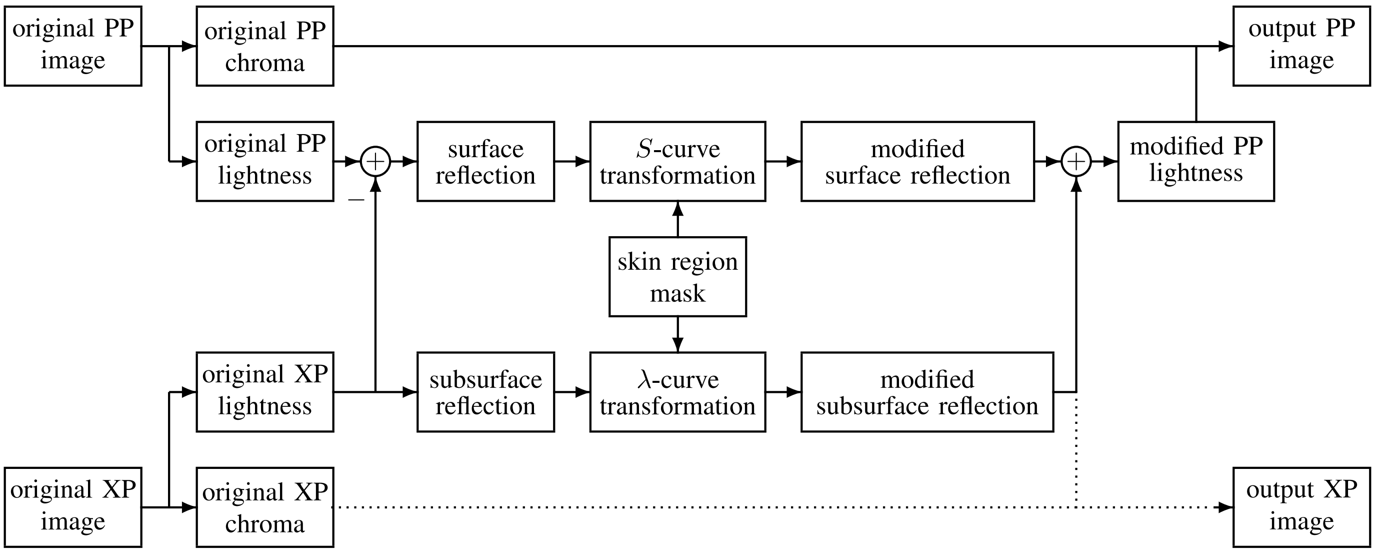

Fig. 4: Surface reflection (SurfRefl) manipulation and subsurface reflection (SubSurfRefl) manipulation

(a) original PP image (b) skin region mask (c) subsurface reflection (d) modified subsurface refl. (e) output XP image (f) surface reflection (g) modified surface refl. (h) output PP image

Fig. 5: Example of surface and subsurface reflection manipulation, using λ-curve for subsurface reflection and S-curve for surface reflection

skin age effects. Each original image was accompanied by 10 modified images with varying surface reflections ($S = 1/3, 1/2.6, 1/2.2, 1/1.8, 1/1.4, 1.4, 1.8, 2.2, 2.6, 3$) and fixed subsurface reflection ($\lambda = 1$). Thus, for each subject, each condition, and each level, there were 11 images. The resulting skin gloss covers a broad range that is representative of real use cases. However, as we mentioned above, the range of our studies did not cover all the possibilities. Table I summarizes the stimuli for the two studies. A complete set of images for one subject at the two scales (entire face and image patch) is shown in Figures 6 and 7. In total, there were 550 macro-scale images with 590×500 pixel resolution in Study 1A, and 264 meso-scale images with 256×256 pixel resolution in Study 1B.

2) Apparatus: As we mentioned in Section II, all images were captured using a VISIA-CR 4.1 camera/lighting system, which uses broad spectrum daylight illumination. We should point out that changing the camera, filters, or illumination would require recalibration of the system. Study 1A (macro-scale) was conducted with printed images because, due to the limited size of the LCD screen, it was impossible to display multiple macro-scale images on the screen at full resolution. The images were printed with an Epson SureColor P7000 24 inch printer on $5 \times 7''$ Epson Premium Luster Photo Paper at 720 pixels per inch (ppi). We used luster paper, which is between glossy and matte, to make sure that no extra gloss was introduced by the paper. The print quality is claimed to rival that of traditional silver halide prints. For each trial, 22 photos were pinned on a $40 \times 30''$ matte canvas.

Study 1B (meso-scale) was conducted using a calibrated liquid crystal display (LCD), with 1920×1080 resolution. The display was gamma linearized and color calibrated using the Lagom LCD monitor test.[1] The viewing distance was approximately 600 mm, so that a 256 pixel image subtended an angle of 9.39 degrees.

3) Procedure: The macro-scale and meso-scale studies were conducted separately. For each macro-scale trial, each participant was shown a group of 22 images pinned on a matt canvas in random order, and was instructed to re-rank the images in order of increasing visual gloss. All of the 22 images in a group came from the same subject, 11 before cleansing (1 original and 10 varying SurfRefl) and 11 after cleansing (1 original and 10 varying SurfRefl). The meso-scale trials were conducted in a similar fashion, and the only difference was that the patches were shown on the LCD display, and a mouse cursor was used to drag and drop each image to the desired ranking position. For both studies, skin gloss was explained as “a shiny or radiant appearance of human skin.”

4) Participants: The two studies were conducted with 10 participants, eight female and two male with normal or corrected-to-normal vision. Before the study, all participants

[1] http://www.lagom.nl/lcd-test/

Fig. 6: Examples of macro-scale side-viewed stimuli for Study 1

TABLE II: Visual Stimuli for Empirical Study 2

		Macro-scale	**Meso-scale**
Facial skin subjects		6	48
Conditions	Lighting	PP	PP
	Viewing	Side	Side
	Cleansing	Before	Before
Each condition: 9 images (1 orig. + 8 modified SubSurfRefl)			
Each trial: 2 images of ONE skin subject in ONE view			

were asked to read and sign consent forms.

B. Study 2: Gloss perception versus subsurface reflection

The second set of studies was intended to determine the influence of the subsurface reflection and was conducted with fixed surface reflection.

1) Visual Stimuli: The visual stimuli for Study 2A included images of 6 subjects at the macro-scale level, and the stimuli for Study 2B included 48 skin image patches at the meso-scale level. The stimuli for both studies consisted of side view, original and modified PP images of facial skin, in one skin condition (before cleansing). Each original image was accompanied by 8 modified images with varying subsurface reflections ($\lambda = 1/1.4, 1/1.3, 1/1.2, 1/1.1, 1.1, 1.2, 1.3, 1.4$) and fixed surface reflection ($S = 1$). Thus, for each subject, each condition, and each level, there were 9 images. Since the λ-curve transformation changes the lightness of the image, the modified images covered a broader (realistic but not exhaustive) range of complexions than those of the subjects in our study. Table II summarizes the stimuli for the two studies. A complete set of images for one subject at the two scales (entire face and image patch) is shown in Figures 8 and 9. In total, there were 54 macro-scale images with 590×500 pixel resolution in Study 2A, and 432 meso-scale images with 256×256 pixel resolution in Study 2B.

2) Apparatus: The tests were all conducted using a calibrated LCD screen with the same settings as in Study 1B.

Fig. 7: Examples of meso-scale stimuli (side view) for Study 1

3) Procedure: In Studies 2A and 2B, we used forced alternative choice (2AFC) tests instead of the re-ranking tests. This was possible because in this study there were only 9 images to be ranked, compared with 22 in the fist study, thus drastically reducing the number of paired comparisons. By showing only two images at a time, the users were not exposed to the entire set of stimuli, which ranged from light to dark complexion, thus reducing the risk that they confuse the task of gloss perception with that of brightness perception. For each scale, the participants were shown two images of the same subject with different subsurface reflections, and were asked to select the one that appeared glossier. The images were shown side by side, and the participants could use the left/right arrow buttons in a standard keyboard to toggle between the two stimuli and the spacebar to finalize their selection and to advance to the next pair.

4) Participants: The participants were the same as those in Studies 1A and 1B.

IV. Empirical Studies: Analysis of the Results

Since the visual information at the macro-scale and the meso-scale levels is substantially different, we will rely on different features to analyze the two scales. As a result, the discussion is organized according to scale, as opposed to surface and subsurface component in the previous section.

A. Macro-scale Analysis

We conducted separate investigations of the influence of surface and subsurface reflection on gloss perception, but the methods are similar. To analyze the participant evaluations in the two empirical studies, we rely on Thurstonian Scaling [23], [24], as the model does not only apply to paired comparison data, but also works for ranking data as well by transforming rankings into paired comparisons. The model assumes that the relative magnitudes of the preferences for the stimuli can be determined by the winning frequencies that one stimulus is selected over another. When the winning frequency was too small ($< .02$) or too large ($> .98$) to give stable estimates, the values in the preference matrix were omitted and treated as missing values [25]. We then applied the Thurstone Case V model to convert pairwise preferences to continuous perception scores. The scores were further normalized to Z-scores to facilitate evaluation across the 25 subjects. Note that in the study of surface reflection, the stimuli contain two facial conditions (before and after cleansing). As shown in Table III, for each subject, the perceived gloss (Z-score) of a face after cleansing is lower than the corresponding face before cleansing. The difference between the two conditions is calculated as the relative gloss reduction for each subject. The perceived gloss was on average reduced by 46.2% (with error bar $\pm 12.37\%$) after skin cleansing across all 25 subjects.

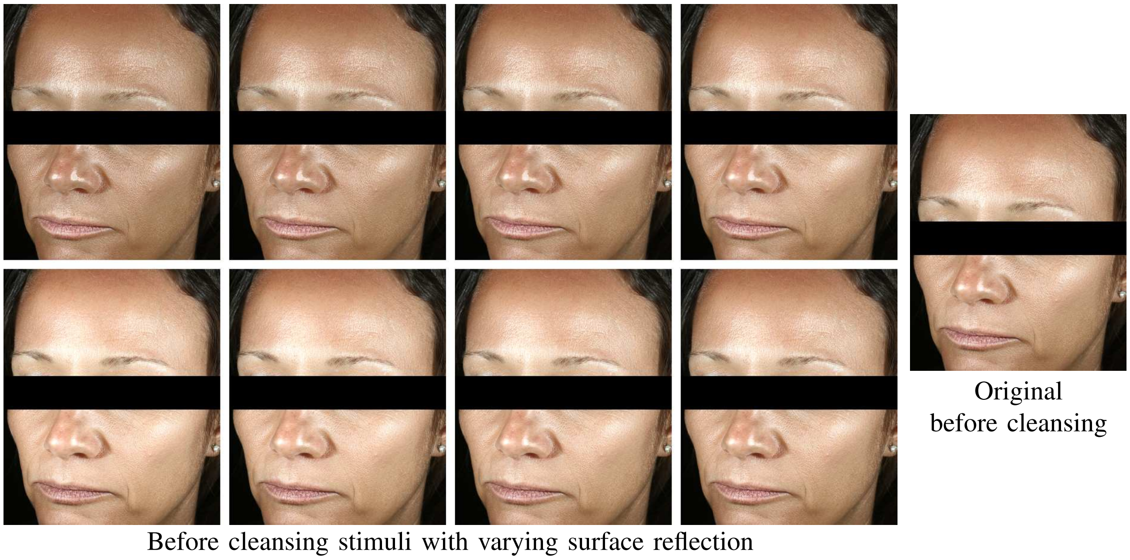

Fig. 8: Examples of macro-scale side-viewed stimuli for Study 2

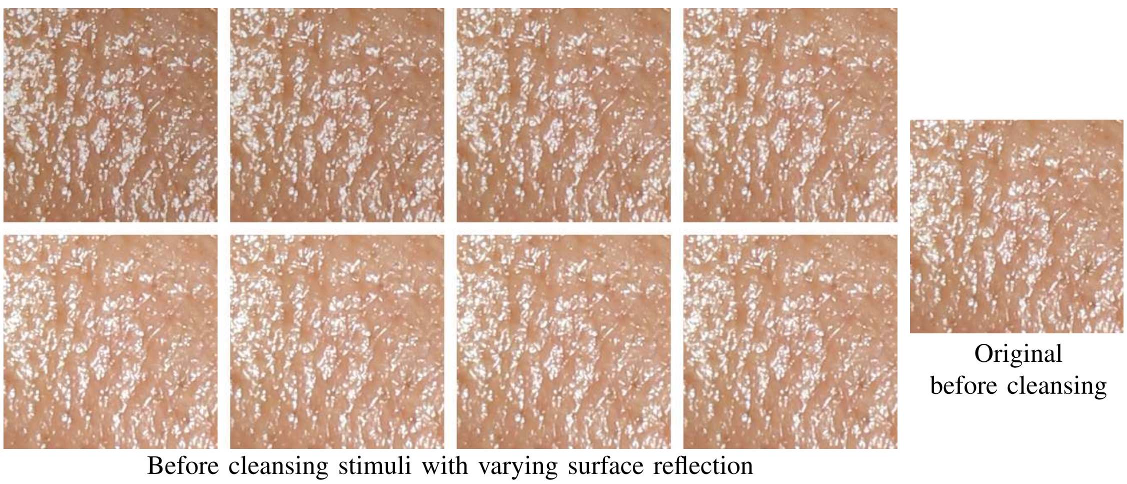

Fig. 9: Examples of meso-scale stimuli (side view) for Study 2

The relative gloss perception of the two conditions is also displayed in Figure 10. The relative gloss is the position of the Z-score of the specific image as to the Z-score range of all available images of the same subject.

To analyze the relationship between surface reflection and gloss perception, we calculated the *mean, standard deviation, skewness, and kurtosis* of the surface and subsurface reflection images, for a total of 8 image statistics. The results of the perceived gloss (Z-score) versus the surface statistics are plotted in Figure 11 across all subjects. For better visualization, the statistics of each subject were normalized by subtracting the mean and dividing by the standard deviation. The circled data points in each plot of Figure 11 are the before and after cleansing original images of Subject ID:009. Similarly, the results of perceived gloss (Z-score) versus subsurface statistics are plotted in Figure 12 across all subjects.

The Spearman correlations of each statistic and the p-value are summarized in Table IV. It is no surprise that different statistics show different correlations with gloss perception. For example, the mean lightness of the surface reflection has positive correlation with gloss perception because it relates to the specular coverage on the skin surface, while the mean lightness of the subsurface reflection correlates negatively with gloss perception because it relates to the skin complexion. On the other hand, the skewness of the surface reflection has negative correlation with gloss perception, while the opposite is true for the subsurface reflection. There does not appear to be an obvious interpretation of this result, and seems consistent with the skepticism that a simple skewness hypothesis can account for overall gloss perception [15], [16]. The standard deviation of both the surface and subsurface reflections is positively correlated with gloss perception, while the kurtosis of both reflections is negatively correlated with gloss perception; this is not surprising because high variance and low kurtosis signify a wider spread of lightness values that results in increased contrast, which is correlated with gloss [12].

As the perception of macro-scale level skin gloss is affected by both surface and subsurface statistics, we concatenated the statistics of the surface and subsurface reflection images (total of 8 statistics) and learned a linear regression to predict relative gloss difference. As a comparison, we also learned a linear regression model based on the 4 statistics (mean,

TABLE III: Macro-scale perceived gloss of each subject before and after cleansing

subject ID	001	002	003	004	005	006	007	008	009	010	011	012	013
Z-score before cleansing	0.31	0.27	0.26	0.31	0.18	0.47	0.46	0.40	0.55	0.37	0.42	0.34	0.31
Z-score after cleansing	-0.38	-0.49	-0.54	-0.96	-0.28	-0.67	-0.68	-0.77	-0.77	-0.43	-0.68	-0.33	-0.21
relative gloss reduction (%)	35.0	39.7	43.1	64.4	25.6	55.5	55.5	57.6	59.1	40.7	56.5	36.4	30.5
subject ID	014	015	016	017	018	019	020	021	022	023	024	025	
Z-score before cleansing	0.39	0.37	0.17	0.33	0.20	0.77	0.69	0.28	0.11	0.24	0.35	0.36	
Z-score after cleansing	-0.69	-0.40	-0.51	-0.68	-0.44	-0.88	-0.69	-0.70	-0.32	-0.26	-0.68	-0.66	
relative gloss reduction (%)	53.5	38.7	38.1	52.3	34.5	67.3	61.8	50.0	28.8	26.8	51.9	51.9	

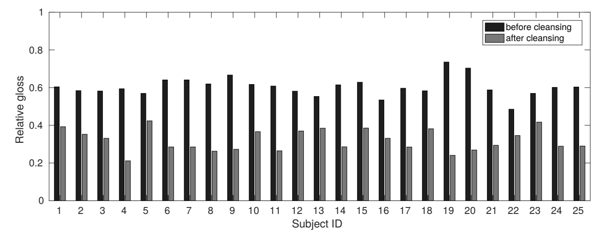

Fig. 10: Macro-scale perceived gloss (as to the gloss range) of each subject in before and after cleansing condition

TABLE IV: Correlation between surface and subsurface statistics and gloss perception

	surface reflection		subsurface reflection	
Statistic	Correlation	p-value	Correlation	p-value
mean	0.855	< 0.001	-0.938	< 0.001
std.	0.953	< 0.001	0.914	< 0.001
skewness	-0.661	0.034	0.934	< 0.001
kurtosis	-0.818	< 0.001	-0.654	0.005

standard deviation, skewness, and kurtosis) extracted from the overall reflection map (single modality) of each skin image. Figure 13 shows how the predicted results of the two models aligned with the results of human judgments. With 10-fold cross validation, the RMSE of single image statistics is 1.69, while the RMSE of the combined statistics of the surface and subsurface reflation images is 0.403, a considerable performance improvement. Thus, our analysis demonstrates that the perceived gloss difference can be predicted quite reliably from a combination of statistics extracted from the surface and subsurface reflections, while relying on unpolarized light to obtain the overall reflection is considerably less effective at predicting gloss.

B. Meso-scale Analysis

As in the analysis of macro-scale gloss, we applied Thurstonian Scaling to estimate the perceived gloss scores of skin patches. Table V lists the perceived gloss (Z-score) for each skin patch before and after cleansing. The perceived gloss was on average reduced by 19.75% (with error bar $\pm 16.20\%$) after skin cleansing across all 24 skin patches. The relative gloss perception of the two conditions is also displayed in Figure 14.

Compared to the relative gloss reduction at the macro-scale (Table III and Figure 10), the meso-scale gloss reduction is on average smaller and has larger variance.

In contrast to the macro-scale, where we extracted statistics in the image domain, for the meso-scale we extracted statistics in the subband domain, which is more appropriate for texture patches that have more or less spatially uniform statistical characteristics, as opposed to the spatially varying characteristics of the macro-scale images. For the subband analysis we used a raised cosine-log filter bank proposed by Peli [26]:

$$G_k(f) = \begin{cases} 0.5 + 0.5\cos(\pi \log_2 f - \pi k), & \text{if } 2^{k-1} < f < 2^{k+1} \\ 0, & \text{otherwise.} \end{cases} \tag{4}$$

Here f is the spatial frequency. An 256×256 pixel image can be divided into eight subbands (scales) with peak spatial frequencies at 1, 2, 4, 8, 16, 32, 64 and 128 cycles per picture (cpp).

For each subband of the surface and subsurace reflection, apart from the image moments (mean, standard deviation, skewness, and kurtosis), we calculated the autocorrelation, entropy, and local homogeneity [27], [28]. Note that the mean of all the subbands, except the lowpass, is zero. Thus, there are 12 statistics for each subband, while the mean of the surface and subsurface reflections was calculated in the image domain. The total number of statistics is 98.

Figure 15 plots the correlation between subband statistics (surface and subsurface) and meso-scale level gloss scores. Apart from the standard deviation, the statistics of the surface reflection (Figure 15a) do not have obvious correlation (between -0.5 and +0.5) with gloss perception at low frequency bands (center frequency 1, 2, and 4 cpp). The correlation becomes stronger with gloss perception at higher subband frequencies (center frequency 16, 32, 64 cpp). Compared to the obvious statistical relationship in the surface reflection, the correlation values of the subsurface reflection statistics (Figure 15b) are not that strong. Apart from skewness, for

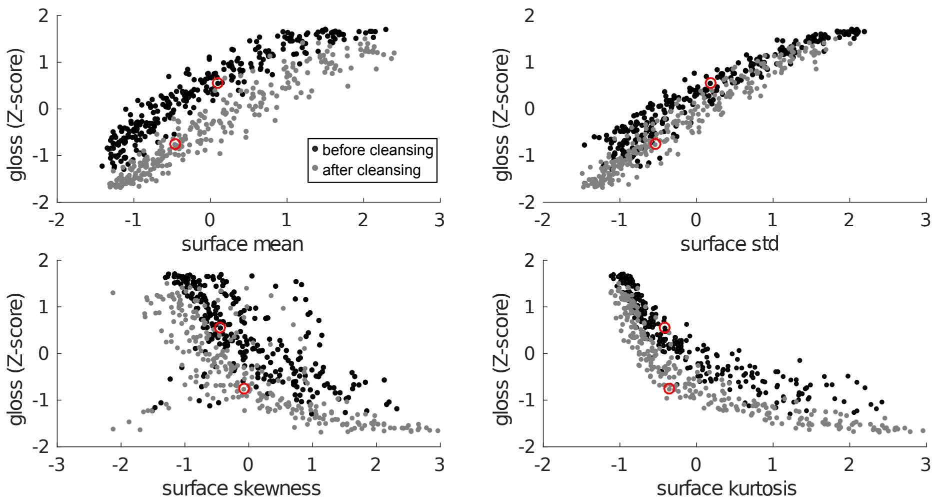

Fig. 11: Macro-scale perceived gloss versus surface statistics. The x-axis shows the normalized statistics of the surface reflection and the y-axis shows the normalized gloss scores after Thurstonian scaling. The circled points are the two original images of one subject.

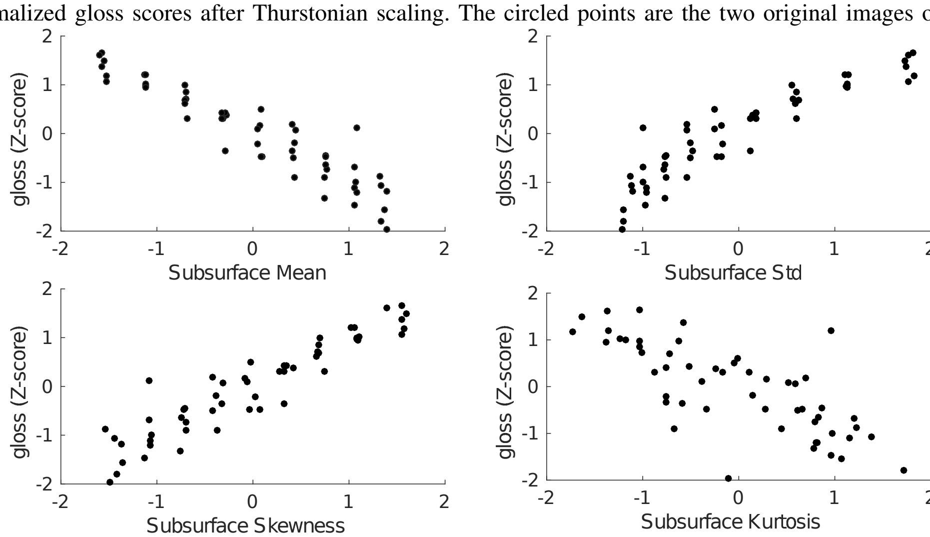

Fig. 12: Macro-scale perceived gloss versus subsurface statistics. The x-axis represents the normalized statistics of the subsurface lightness component and the y-axis represents the normalized gloss scores after Thurstonian scaling.

which the correlation is stronger at lower subband frequencies, most values are between -0.5 and 0.5. One possible reason is that the subsurface reflection does not contain much variation in surface geometry. As can be seen in the example of Figure 1, the skin relief (wrinkles, pores) is more apparent in the surface reflection than in the subsurface reflection.

We then used the 98 subband statistics as features for predicting gloss differences at the meso-scale level. Since the statistics across subband are not independent, a simple linear regression cannot work well when faced with the collinearity problem. Therefore, we chose partial least square (PLS) regression to analyze the multiple subband statistics, and the learned variable importance in the projection (VIP) of each parameter serves as a criterion for assessing the importance of each variable. The larger the value of VIP, the more important the corresponding variable. Table VI lists the VIP values of each of the subband statistics in the regression model. We used 1.0 as a threshold for selecting statistical features for the final model. For comparison, we also fit PLS regression to the 14 statistics obtained directly from the surface and subsurface reflection images without subband analysis. Figure 16 shows how the predicted results align with the perceived gloss using statistics of the surface and subsurface reflections with and without subband analysis. Without subband analysis, the RMSE of the model fitting is 0.547. When a concatenation of subband stististics is used, the RMSE value of the model fitting is reduced to 0.209.

C. Macro-scale versus Meso-scale

Our analysis demonstrates that at both scales a combination of statistics extracted from the surface and subsurface reflections can reliably predict gloss perception. For the macro-scale analysis we relied on image domain statistics, while for the meso-scale analysis we found that subband statistics result in more reliable prediction. This is because the macro-scale encompasses information from the entire face, while the meso-scale is restricted to localized and more detailed patches of spatially uniform texture.

The selection of appropriate scale depends on the application. When overall appearance is the primary concern, then macro-scale is the obvious choice. When more localized or

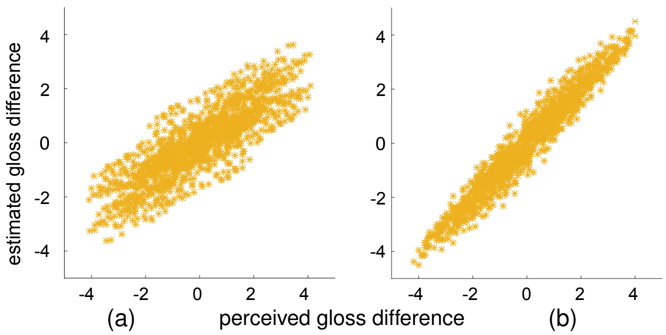

Fig. 13: Macro-scale Gloss: Prediction of relative gloss difference using statistical features extracted from (a) overall reflection (b) combination of separate surface and subsurface reflection images.

specialized information is needed, then meso-scale is preferable.

V. Discussion

The main goal of the present study was to develop statistical models that characterize the relationship between surface and subsurface reflections and skin gloss perception. Since human facial skin involves variations in multiple dimensions across different subjects that are difficult to control, we considered the simplified task of within-subject gloss estimation.

We conducted separate empirical studies and analysis for gloss perception at the macro-scale (whole face) and the meso-scale (skin patch) level, as the two levels present different kinds of information. We built a database of facial skin images using polarization photography, and enriched the appearance variations by modifying the surface and subsurface reflection components using photometric transformations. In addition to providing additional data for exploring the relationship between image statistics and gloss perception, the photometric transformations enable "digital makeup," that is, make it possible to change the complexion and to enhance or reduce the gloss of a face or skin patch.

Our empirical studies confirm that skin gloss perception is affected by both the surface and subsurface reflections. Our analysis demonstrates that perceived gloss depends on a combination of statistics extracted from the surface and subsurface reflections, and confirm that simple image statistics like skewness cannot fully represent the perception of gloss [15], [16].

In the study of macro-scale level gloss, we found that the surface and subsurface reflection components have different effects on perceived gloss, with the corresponding statistics sometimes exhibiting opposite correlation with the perceived gloss score. Our results show that perceived gloss has a positive correlation with the mean and standard deviation, and negative correlation with the skewness and kurtosis of the surface reflection. This is consistent with the findings of Marlow *et al.* [29] on synthesized images, who demonstrated the importance of specular coverage, strength, and sharpness for gloss perception. It also demonstrates that the skewness hypothesis [14] does not hold for the surface reflection. Our results also show that, for fixed surface reflection, darker complexion (subsurface reflection) is perceived as glossier. Finally, we have shown that a linear regression model that concatenates surface and subsurface statistics provides an excellent prediction of gloss (0.4 RMSE), which considerably outperforms the model that is based only on the statistics of the lightness image (1.7 RMSE).

In the study of meso-scale level gloss, we separated each reflection component into subband images and used partial least squares regression to calculate the importance of each statistic extracted from each subband. We found that with the exception of the skewness of the subsurface component, the subband statistics at higher frequencies generally show stronger contribution (larger variable importance in the projection value) to perceived gloss than those at lower frequencies.

We also considered the differences in perceived gloss before and after cleansing, and found that at the macro-scale there is a significant reduction in perceived gloss after cleansing, while the effect is weaker at the meso-scale, which confirms the fundamental differences between the two scales.

The studies we have presented are limited to the perception of images of the same subject, and as such, are not sufficient for developing a global gloss perception scale. In our future work we plan to extend the current within-subject gloss perception to a global range of gloss perception. We also plan to conduct studies with subjects that cover a broader range of skin tones, and to study the effects of a variety of cosmetics beyong basic cleansing.

References

[1] J. Middleton, "The mechanism of water binding in stratum corneum," *British J. Dermatology*, vol. 80, no. 7, pp. 437–450, 1968.

[2] J. S. Koh, H. Kang, S. W. Choi, and H. O. Kim, "Cigarette smoking associated with premature facial wrinkling: image analysis of facial skin replicas," *Int. J. Dermatology*, vol. 41, no. 1, pp. 21–27, 2002.

[3] A. Raitio, J. Kontinen, M. Rasi, R. Bloigu, J. Röning, and A. Oikarinen, "Comparison of clinical and computerized image analyses in the assessment of skin ageing in smokers and non-smokers." *Acta dermato-venereologica*, vol. 84, no. 6, 2004.

[4] L. Li, S. Mac-Mary, J.-M. Sainthillier, S. Nouveau, O. De Lacharriere, and P. Humbert, "Age-related changes of the cutaneous microcirculation in vivo," *Gerontology*, vol. 52, no. 3, pp. 142–153, 2006.

[5] A. Jeudy, V. Ecarnot, and P. Humbert, "Measurement of skin radiance," in *Agache's Measuring the Skin: Non-invasive Investigations, Physiology, Normal Constants*, P. Humbert, F. Fanian, H. I. Maibach, and P. Agache, Eds. Springer, 2017, ch. 17, pp. 161–176.

[6] W. Budde, "The calibration of gloss reference standards," *Metrologia*, vol. 16, no. 2, p. 89, 1980.

[7] E. H. Adelson, "On seeing stuff: The perception of materials by humans and machines," in *Human Vision and Electronic Imaging VI*, ser. Proc. SPIE, B. E. Rogowitz and T. N. Pappas, Eds., vol. 4299, San Jose, CA, Jan. 2001, pp. 1–12.

[8] A. Matsubara, Z. Liang, Y. Sato, and K. Uchikawa, "Analysis of human perception of facial skin radiance by means of image histogram parameters of surface and subsurface reflections from the skin," *Skin Res. Technol.*, vol. 18, no. 3, pp. 265–271, 2012.

[9] Y. V. Haeghen, J. M. A. D. Naeyaert, I. Lemahieu, and W. Philips, "An imaging system with calibrated color image acquisition for use in dermatology," *IEEE Trans. Med. Imag.*, vol. 19, no. 7, pp. 722–730, 2000.

[10] M. Baret, N. Bensimon, S. Coronel, S. Ventura, S. Nicolas-Garcia, R. Korichi, and G. Gazano, "Characterization and quantification of the skin radiance through new digital image analysis," *Skin Res. Technol.*, vol. 12, no. 4, pp. 254–260, 2006.

[11] H. Tanaka, G. Nakagami, H. Sanada, Y. Sari, H. Kobayashi, K. Kishi, C. Konya, and E. Tadaka, "Quantitative evaluation of elderly skin based on digital image analysis," *Skin Res. Technol.*, vol. 14, no. 2, pp. 192–200, 2008.

TABLE V: Meso-scale perceived gloss of each subject in before and after cleansing condition

subject ID	001	002	003	004	005	006	007	008	009	010	011	012	013
Z-score before cleansing	0.10	0.45	0.21	0.12	0.16	0.48	0.26	0.21	0.45	0.25	0.41	0.30	0.24
Z-score after cleansing	-0.14	-0.07	0.16	0.10	0.10	-0.87	-0.31	0.04	-0.58	-0.27	0.07	0.20	0.03
relative gloss reduction (%)	13.8	23.9	2.5	1.1	3.4	60.8	27.5	9.3	49.4	28.4	15.2	5.2	11.9

subject ID	014	015	016	017	018	019	020	021	022	023	024	025
Z-score before cleansing	0.12	0.19	0.16	0.22	0.55	0.20	0.39	0.40	0.19	0.65	0.35	
Z-score after cleansing	0.05	-0.08	-0.57	0.04	-0.03	-0.06	-0.22	0.21	0.04	-0.50	-0.01	
relative gloss reduction (%)	3.5	14.5	36.8	10.6	26.6	15.2	28.7	8.7	7.9	49.7	19.3	

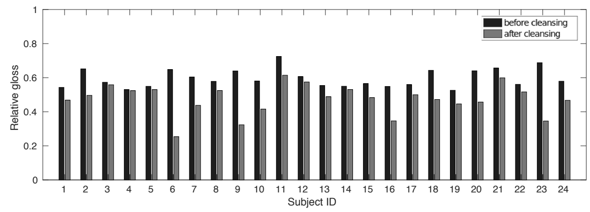

Fig. 14: Meso-scale perceived gloss (as to the gloss range) of each subject in before and after cleansing condition

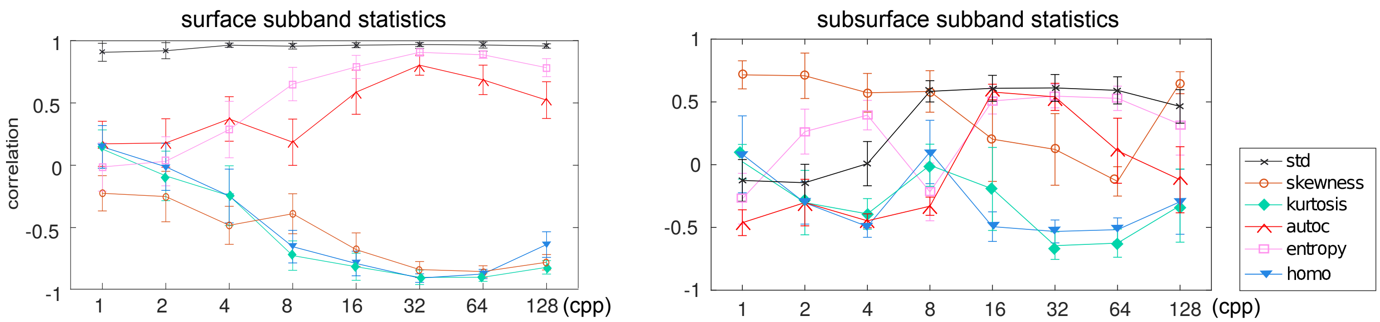

Fig. 15: Correlation of subband statistics with meso-scale gloss scores. Error bars are the standard error of the mean across all skin patches.

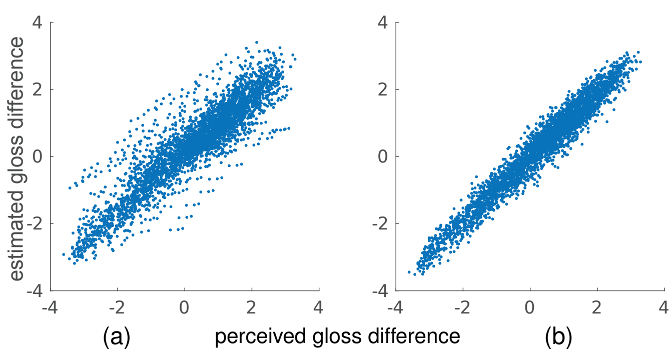

Fig. 16: Meso-scale Gloss: Prediction of relative gloss difference using statistical features extracted from (a) surface and subsurface reflection (b) subbands of surface and subsurface reflection images.

[12] J. Wang, T. N. Pappas, and H. de Ridder, "Effects of contrast adjustment on visual gloss of natural textures," in *Human Vision Electr. Imaging XX*, ser. Proc. SPIE, B. E. Rogowitz, T. N. Pappas, and H. de Ridder, Eds., vol. 9394. San Francisco, CA: Int. Soc. Optics Photonics, Feb. 2015, pp. 93 940F–1–11.

[13] M. W. A. Wijntjes and S. C. Pont, "Illusory gloss on Lambertian surfaces," *J. Vision*, vol. 10, no. 9, pp. 1–12, 2010.

[14] I. Motoyoshi, S. Nishida, L. Sharan, and E. H. Adelson, "Image statistics and the perception of surface qualities," *Nature*, vol. 447, pp. 206–209, May 2007.

[15] B. L. Anderson and J. Kim, "Image statistics do not explain the perception of gloss and lightness," *J. Vision*, vol. 9, no. 11, pp. 10–10, 2009.

[16] J. Kim and B. L. Anderson, "Image statistics and the perception of surface gloss and lightness," *J. Vision*, vol. 10, no. 9, pp. 3–3, 2010.

[17] P. J. Marlow, J. Kim, and B. L. Anderson, "The perception and misperception of specular surface reflectance," *Current Biology*, vol. 22, no. 20, pp. 1909–1913, 2012.

[18] Y.-X. Ho, M. S. Landy, and L. T. Maloney, "Conjoint measurement of gloss and surface texture," *Psychological Science*, vol. 19, no. 2, pp. 196–204, Feb. 2008.

[19] L. Qi, M. J. Chantler, J. P. Siebert, and J. Dong, "The joint effect of mesoscale and microscale roughness on perceived gloss," *Vision research*, vol. 115, pp. 209–217, 2015.

[20] C. B. Wiebel, M. Toscani, and K. R. Gegenfurtner, "Statistical correlates of perceived gloss in natural images," *Vision Res.*, vol. 115, pp. 175–187, 2015.

[21] X. Xiong and F. De la Torre, "Supervised descent method and its applications to face alignment," in *IEEE Int. Conf. Comp. Vision Patt. Recognition (CVPR)*. Pittsburgh: IEEE, 2013, pp. 532–539.

[22] W. R. Tan, C. S. Chan, P. Yogarajah, and J. Condell, "A fusion approach for efficient human skin detection," *IEEE Trans. Industrial Informatics*, vol. 8, no. 1, pp. 138–147, 2012.

[23] L. L. Thurstone, "A law of comparative judgment." *Psychological review*, vol. 34, no. 4, p. 273, 1927.

[24] ——, "Rank order as a psycho-physical method." *Journal of Experimental Psychology*, vol. 14, no. 3, p. 187, 1931.

[25] A. L. Edwards, *Techniques of attitude scale construction*. Ardent Media, 1983.

[26] E. Peli, "Contrast in complex images," *JOSA A*, vol. 7, no. 10, pp. 2032–2040, 1990.

[27] R. M. Haralick, K. Shanmugam, *et al.*, "Textural features for image classification," *IEEE Trans. Syst., Man, Cybern.*, no. 6, pp. 610–621, 1973.

[28] L.-K. Soh and C. Tsatsoulis, "Texture analysis of SAR sea ice imagery using gray level co-occurrence matrices," *IEEE Trans. Geoscience Remote Sensing*, vol. 37, no. 2, pp. 780–795, 1999.

[29] P. J. Marlow and B. L. Anderson, "Generative constraints on image cues for perceived gloss," *J. Vision*, vol. 13, no. 14, pp. 2–2, 2013.

TABLE VI: VIP of subband statistics in PLS regression analysis. Values with larger importance (> 1.0) shown in boldface.

Reflection	Statistics	Center Frequency (cpp)							
		1	2	4	8	16	32	64	128
Surface	mean	**1.31**							
	std	**1.32**	**1.34**	**1.40**	**1.39**	**1.40**	**1.41**	**1.41**	**1.40**
	skewness	0.40	0.38	0.69	0.62	**1.05**	**1.21**	**1.23**	**1.13**
	kurtosis	0.27	0.19	0.53	1.04	**1.18**	**1.29**	**1.29**	**1.18**
	entropy	0.12	0.07	0.51	0.93	**1.13**	**1.30**	**1.27**	**1.12**
	autocorrelation	0.33	0.27	0.55	0.41	0.87	**1.15**	**0.98**	0.76
	homogeneity	0.29	0.14	0.54	0.94	**1.13**	**1.30**	**1.25**	0.92
Subsurface	mean	**1.19**							
	std	0.84	0.73	0.78	**1.15**	**1.21**	**1.22**	**1.17**	0.89
	skewness	**1.09**	**1.06**	**1.09**	0.88	0.98	0.97	0.92	0.95
	kurtosis	0.56	0.83	0.71	0.97	0.85	**1.15**	**1.11**	**1.46**
	entropy	0.97	0.71	0.90	0.49	**1.12**	**1.21**	**1.17**	0.93
	autocorrelation	1.07	0.95	1.51	0.83	**1.33**	**1.21**	0.25	**1.19**
	homogeneity	0.46	0.70	1.13	0.39	**1.10**	**1.18**	**1.15**	0.81

TABLE VII: p-value of each subband statistic with gloss perception

Reflection	Statistics	Center Frequency (cpp)							
		1	2	4	8	16	32	64	128
Surface	mean	< 0.001							
	std	0.003	< 0.001	< 0.001	< 0.001	< 0.001	< 0.001	< 0.001	< 0.001
	skewness	0.31	0.26	0.13	0.14	0.08	0.001	0.002	0.004
	kurtosis	0.35	0.27	0.13	0.05	0.04	< 0.001	< 0.001	< 0.001
	entropy	0.39	0.27	0.11	0.05	0.01	< 0.001	< 0.001	0.008
	autocorrelation	0.25	0.24	0.16	0.37	0.12	0.005	0.006	0.16
	homogeneity	0.30	0.26	0.16	0.04	0.01	< 0.001	< 0.001	0.05
Subsurface	mean	< 0.001							
	std	0.27	0.30	0.19	0.15	0.15	0.16	0.17	0.29
	skewness	0.34	0.32	0.19	0.21	0.14	0.16	0.22	0.29
	kurtosis	0.34	0.24	0.26	0.28	0.13	0.05	0.02	0.05
	entropy	0.30	0.23	0.09	0.21	0.01	0.02	0.01	0.08
	autocorrelation	0.07	0.09	0.02	0.14	0.04	0.01	0.28	0.03
	homogeneity	0.33	0.23	0.03	0.19	0.01	0.01	0.01	0.15

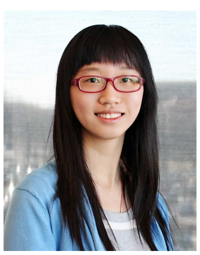

Jing Wang Jing Wang received the Bachelor Degree in Information Engineering from Zhejiang University, China in 2012 and the Ph.D. degree in Electrical Engineering from Northwestern University, Evanston, IL, in 2018. She is currently employed as an AI research scientist at Bloomberg LP, New York, NY. Her research interests include human perception on visual texture, color perception, information retrieval, and entity analysis.

Carla Kuesten receive the B.S. degree from the University of Idaho in 1981, the M.S. degree from Oregon State University in 1983, and the Ph.D. degree from Cornell University in 1992. Dr. Kuesten has 30+ years of experience in sensory and consumer research; she establishes and implements strategic direction for research and conducts global basic and applied qualitative and quantitative research studies. Her recent research focus is on applying perceptual scaling and discrimination methods. She has held numerous positions over the years in the personal care and food industries as well as consulting businesses including: S. C. Johnson Wax, The Institute for Perception, Ocean Spray Cranberries, Arthur D. Little/TIAX, and Amway. Dr. Kuesten is a member of Institute of Food Technologists (IFT), Society of Sensory Professionals (SSP), Sensometrics, Product Development Management Association (PDMA), and American Society for Testing and Materials (ASTM) International.

Jim Mayne received the B.S. degree in physical science from Lyman Briggs College, Michigan State University in 1975. He has worked as scientist at Skin Care PD at Amway (1975-1988), director of Skin Care PD at Matrix Essentials (1988-1990), and principal research scientist for advanced imaging and measure at Amway Corporation, Ada Michigan (1990-2017). He is currently technical consultant at Integral Consultancy, LLC. His interests are in skin care product development, 2D, 3D, and IR imaging, bioinstrumentation for skin research and claims support.

Gopa Majmudar received the M.S. and Ph.D. degrees in microbiology from M. S. University of Baroda, India, in [year] and [year], respectively. She received the prestigious Jawaharlal Nehru Award (gold medal) from the Government of India for her doctoral dissertation research. She is currently working at the Cosmetic science, College of Pharmacy and Pharmaceutical Sciences, University of Toledo, Toledo, OH, USA as a part time faculty. She has worked as a scientist, Faculty member and manager and in scientific advisory boards at academic institutions, Universities and personal care companies such as National Institute of Health (NIH), Bethesda, MD, Institut Jacques Monod, Paris, France, Howard Hughes Medical Institute, University of Michigan, Ann Arbor, Mary Kay, Alberto Culver and Amway in the R&D Department. There, she was actively involved in Cancer research, anti-aging and skin pigmentation research.

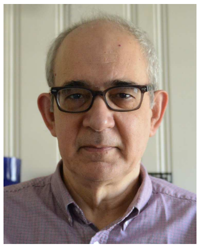

Thrasyvoulos N. Pappas (M'87, SM'95, F'06) received the S.B., S.M., and Ph.D. degrees in electrical engineering and computer science from MIT in 1979, 1982, and 1987, respectively. From 1987 until 1999, he was a Member of the Technical Staff at Bell Laboratories, Murray Hill, NJ. In 1999, he joined the ECE Department at Northwestern University. His research interests are in human perception and electronic media, and in particular, image quality and compression, image analysis, content-based retrieval, model-based halftoning, and tactile and multimodal interfaces. Prof. Pappas is a Fellow of SPIE and IS&T. He has served as Editor-in-Chief of the IEEE Transactions on Image Processing, Vice President-Publications for the Signal Processing Society (SPS) of IEEE, and co-chair of SPIE/IS&T Human Vision and Electronic Imaging Conference. He is currently Editor-in-Chief of the IS&T Journal of Perceptual Imaging.